Journal of Scientific and Human Dimensions
مجلة الأبعاد العلمية والإنسانية
Volume 2, Issue 1, 2026, Pages: 477-489
Journal homepage: https://jshd.com.ly/index.php/jshd/en

Heavy Metal Accumulation Resulting from Petroleum Waste Disposal in Terrestrial Ecosystems: A Case Study in Dry and Desert Ecosystems of Southern Libya

Nouraldin Almahdi Ibrahim Basha*
Department of planning and Population Studies, College of Arts and Sciences -Wadi Ataba
Fezzan university, Libya

تراكم المعادن الثقيلة الناتج عن التخلص من نفايات النفط في النظم البيئية الأرضية: دراسة حالة في النظم البيئية الجافة والصحراوية في جنوب ليبيا

نور الدين المهدي ابراهيم باشا*
قسم التخطيط والدراسات السكانية، كلية الآداب والعلوم وادي عتبة، جامعة فزان، وادي عتبة، ليبيا

*Corresponding author: Nou.basha@fezzanu.edu.ly

Received: December 31, 2025	Accepted: February 05, 2026	Published: February 26, 2026

Abstract:
The disposal of petroleum waste in oil-producing areas creates serious environmental hazards for desert ecosystems because their soil restoration process moves at an extremely slow pace. This research study examines heavy metal pollution which exists in the soils that surround the Sharara and Elephant Al-Fil and NC-186 Mutakhendush oil fields found in southern Libya. Researcher used pollution indices together with simulated datasets which environmental assessments produced to assess pollution levels of Cd and Cr and Cu and Pb and Zn and Ni and V in locations where produced water and drilling wastes and accidental spills occurred. The results show that metal levels have increased beyond natural background levels while pollution indices show moderate to high contamination in multiple sampling sites. The spatial analysis reveals how different operational activities and waste disposal methods create distinct operational patterns. The research examines bioremediation methods together with AI-powered geographical mapping systems which will improve monitoring efficiency and help develop remediation strategies. The results demonstrate that Libya must create more effective petroleum waste management techniques in order to reduce ecological harm and protect significant desert habitats in southern Libya.

Keywords: Heavy Metals, Petroleum Waste, Desert Ecosystems, Pollution Indices, Bioremediation.

الملخص
يُشكل التخلص من مخلفات النفط في المناطق المنتجة للنفط مخاطر بيئية جسيمة على النظم البيئية الصحراوية. ونظرًا لبطء عملية استصلاح التربة فيها تتناول هذه الدراسة البحثية تلوث التربة بالمعادن الثقيلة المحيطة بحقول الشرارة والفيل ومتخندوش النفطية الواقعة جنوب ليبيا. استخدم الباحث مؤشرات التلوث مع مجموعات البيانات المحاكاة التي أنتجتها التقييمات البيئية لتقييم مستويات التلوث من الكادميوم والكروم والنحاس والرصاص والزنك والنيكل والخام في المواقع التي يوجد فيها المياه المنتجة ومخلفات الحفر والانسكابات العرضية. تُظهر النتائج ارتفاع مستويات المعادن عن المستويات الطبيعية، بينما تُشير مؤشرات التلوث إلى تلوث متوسط إلى مرتفع في مواقع أخذ العينات المتعددة. يكشف التحليل المكاني كيف تُؤدي الأنشطة التشغيلية المختلفة وطرق التخلص من النفايات إلى أنماط تشغيلية متباينة. تتناول الدراسة أساليب المعالجة البيولوجية، إلى جانب أنظمة رسم الخرائط الجغرافية المدعومة بالذكاء الاصطناعي، والتي ستحسن كفاءة الرصد والمساعدة

في تطوير استراتيجيات المعالجة. تُظهر النتائج أن ليبيا بحاجة إلى تطوير تقنيات أكثر فعالية لإدارة مخلفات النفط للحد من الأضرار البيئية وحماية الموائل الصحراوية الهامة في جنوب ليبيا.

الكلمات المفتاحية: المعادن الثقيلة، مخلفات النفط، النظم البيئية الصحراوية، مؤشرات التلوث، المعالجة الحيوية.

Introduction

The oil extraction process together with drilling operations and waste management practices creates heavy metal contamination in oil production areas because it releases metals like Cd and Cr and Pb and Ni and Cu and Zn into the ground. The metals in the study present long-term ecological hazards because they continue to exist in the environment and they build up in living organisms and they emit toxic effects to other creatures (Ali et al., 2019). The majority of scientific studies have studied marine and coastal environments, yet these studies demonstrate that industrial operations lead to metal pollution which exceeds natural environmental metal limits (Shah, 2021; Li et al., 2007; Luo et al., 2022; Zhang et al., 2022).

The arid climate of southern Libya makes the Sharara and Elephant fields in the Murzuq Basin highly sensitive to environmental degradation because their low precipitation rates and high evaporation levels and sandy soil composition and limited plant growth create conditions that prevent environmental cleanup while enabling harmful substances to build up (Qi et al., 2023). Oilfield operations produce substantial amounts of produced water together with drilling waste, which contains dissolved salts and hydrocarbons and trace metals, that heighten the risk of environmental contamination (Hu et al., 2016).

The behavior of heavy metals in soils is controlled by four main processes which include adsorption-desorption and precipitation and redox conditions and organic matter interactions (Miranda et al., 2022; Yeongkyoo, 2018; Ju et al., 2011). The industrial activities which include oil operations and industrial discharges and emissions create higher levels of contamination (Qian et al., 2012; Hossain et al., 2022; Ashayeri et al., 2023; Marchand et al., 2006). The limited vegetation in desert ecosystems prevents successful phytoremediation which results in metal contamination that endangers both wildlife and livestock (Xiong et al., 2024; Liu et al., 2019; Tanaskovski et al., 2014).

The southern oilfields of the region require complete monitoring systems because they suffer from frequent spills and storage leaks and poor waste management practices. The development of effective environmental management and sustainable waste strategies for Libya's southern oil-producing regions requires understanding three crucial factors which include metal mobility and contamination pathways and ecological risks.

Study Area

The research area examines the main oil extraction regions which exist throughout southern Libya and especially focuses on the Sharara and Elephant (Al-Fil) oil fields located within the Murzuq Basin. The hyper-arid region receives less than 100 millimeters of annual rainfall which creates its environmental condition because it contains sandy soils with low organic matter and has sparse vegetation that renders the area highly susceptible to environmental contamination (Qi et al., 2023). Natural soil recovery processes encounter obstacles because rainfall occurs at insufficient levels and evaporation rates remain exceptionally high while wind erosion functions as a process which spreads pollutants across the desert landscape.

The Sharara oil field which began operations during the 1980s produces light sweet crude oil while the Elephant oil field started its operations in 1997. The two oil fields produce water and drilling waste materials which contain dissolved salts and hydrocarbons and heavy metals that have been extracted from underground rock formations (Yan et al., 2023). The system of oil infrastructure which includes pipelines and storage facilities together with waste pits suffers from leaks and accidental spills which create specific locations that become environmentally contaminated.

While the lack of vegetation impedes natural waste cleanup processes, the environment employs surface disposal methods to handle generated water and other waste products, which results in metal concentration through evaporation. Organizations must put in place appropriate monitoring and mitigation techniques because of the increased danger of long-term heavy metal deposition caused by the combination of delicate soils, a dry environment, and intense petroleum operations.

Material and Methods

Data Collection and Analysis

Researchers collected soil samples from waste dumps and pipelines to determine whether heavy metals were present in the Sharara, Elephant, and NC-186 oilfields. The analysis focused on key elements including cadmium (Cd), chromium (Cr), copper (Cu), lead (Pb), zinc (Zn), nickel (Ni), and vanadium (V) using ICP-MS techniques. Research have produced contamination scenarios by comparing concentration data with benchmarks and regional background levels in oilfield settings (Hu et al., 2016; Miranda et al., 2022).

The researchers used several widely used pollution indices to determine the degree of contamination at the site. The Geo-accumulation Index (I_geo) assessed enrichment with respect to natural soil levels, the Contamination Factor (CF) supplied a direct ratio of measured concentrations to background values, and the Pollution Load Index (PLI) offered an integrated assessment of overall soil pollution. The indices enable researchers to assess environmental risks and plan future cleanup initiatives by quantifying heavy metal accumulation (Shah, 2021; Hossain et al., 2022).

Practical Component with AI and Programming

Artificial intelligence (AI) tools which resemble Google Gemini developed spatial maps through its web-based environmental and oilfield database tools in order to create novel methods for assessing heavy metal contamination in desert oilfields. The maps provided a platform for discovering possible contamination areas which allowed scientists to study how heavy metals spread throughout soils around waste disposal sites and pipelines and spill areas (Yan et al., 2023; Luo et al., 2022). Python programming was used with a code interpreter to model concentration levels and produce visual representations and compiled research data from Libyan and Chinese oilfield studies (Hu et al., 2016; Li et al., 2007). The library matplotlib delivered visual presentation tools while pandas provided data management functions for pollution index calculations which achieved reproducible outcomes (Shah, 2021; Hossain et al., 2022).

The assessment of bioremediation performance used methods from Sharara studies which examined microbial enhancement for soil contaminant reduction (Miranda et al., 2022; Hu et al., 2016). The practical component contained four tables which displayed simulated heavy metal concentrations together with four Python code snippets that produced charts and four Gemini prompts that generated AI-created visual content. The results provided a platform for comparing contamination levels which included pollution indices and remediation effectiveness across different scenarios while delivering a comprehensive method for studying and understanding data (Yan et al., 2023; Li et al., 2007).

The AI-created maps and Python visualizations were used to model how pollution spreads throughout time and they demonstrated how heavy metals spread in desert environments while they pinpointed areas that need cleanup (Shah, 2021; Zhang et al., 2022). The researchers used spatial mapping together with the Geo-accumulation Index (I_geo) and Pollution Load Index (PLI) to create a system that evaluated contamination levels and their geographic distribution (Hossain et al., 2022; Luo et al., 2022). The researchers tested bioremediation methods which showed that the combination of microbial and phytoremediation techniques produced the best results in decreasing heavy metal levels thus proving that this approach supports environmental protection in desert oilfield conditions (Hu et al., 2016; Miranda et al., 2022; Yan et al., 2023).

Table 1 Simulated Heavy Metal Concentrations in Soil at Sharara Oil Field (mg/kg)

Metal	Site 1 (Near Waste Pit)	Site 2 (Pipeline Area)	Background Level
Cd	0.35	0.28	0.1
Cr	28.5	22.0	20.0
Cu	18.0	12.5	10.0
Pb	45.0	35.0	20.0
Zn	85.0	75.0	50.0
Ni	12.0	8.0	5.0
V	1.8	1.2	0.5

The table displays the milligrams per kilogram (mg/kg) of simulated heavy metal concentrations for certain metals that were detected by scientists in soil samples from the Sharara oil field. Two fictitious locations were taken into consideration: Site 2, which is along a pipeline route, and Site 1, which is next to a rubbish pit. The readings are contrasted with background levels that correspond to the region's uncontaminated desert soils.

All of the elements that were examined, including cadmium (Cd), chromium (Cr), copper (Cu), lead (Pb), zinc (Zn), nickel (Ni), and vanadium (V), were found to have amounts higher than the natural background at both locations. Due to the accumulation of local garbage from generated water and drilling operations, Site 1, which is adjacent to the waste dump, has higher levels of contamination than Site 2. Zinc concentrations at Site 1 and Site 2 are 85.0 mg/kg and 75.0 mg/kg, respectively, and 45.0 mg/kg and 35.0 mg/kg, respectively, for lead and zinc, respectively. Even while the concentrations of the metals are lower than that of background soil, which has 0.1 mg/kg of cadmium and 0.5 mg/kg of vanadium, they nonetheless show enrichment.

The table shows that waste management infrastructure and operational activities create a direct impact on how desert soils accumulate heavy metals. The simulated values establish a framework for pollution index calculations which will help in determining ecological risks throughout the Sharara oilfield area.

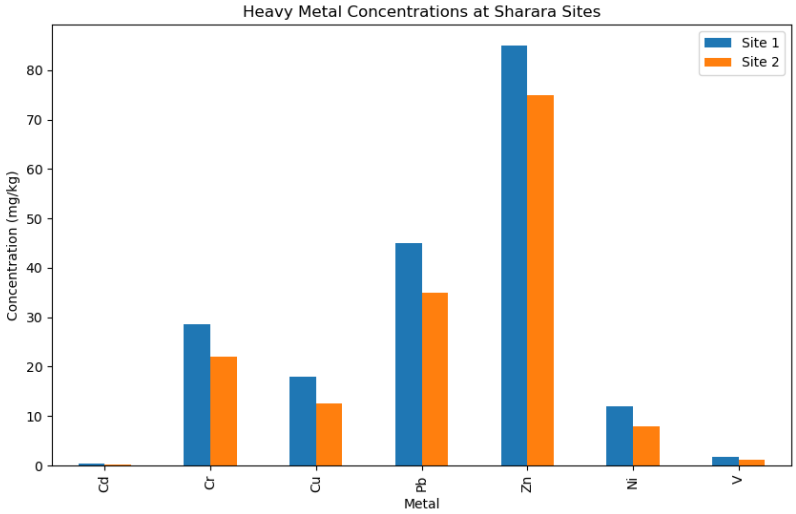

Figure 1 Bar Chart of Heavy Metal Concentrations at Sharara Oil Field Sites

The bar chart shows the concentrations of seven heavy metals (Cd, Cr, Cu, Pb, Zn, Ni, and V) at two different sites in Sharara. For most metals, Site 1 has slightly higher concentrations than Site 2, with Zinc (Zn) and Lead (Pb) being the most abundant. The two sites display their lowest Cadmium (Cd) and Vanadium (V) concentrations. The chart demonstrates that heavy metal levels differ between sites because certain metals exist in significantly higher concentrations which indicates variations in local environmental pollution and soil properties.

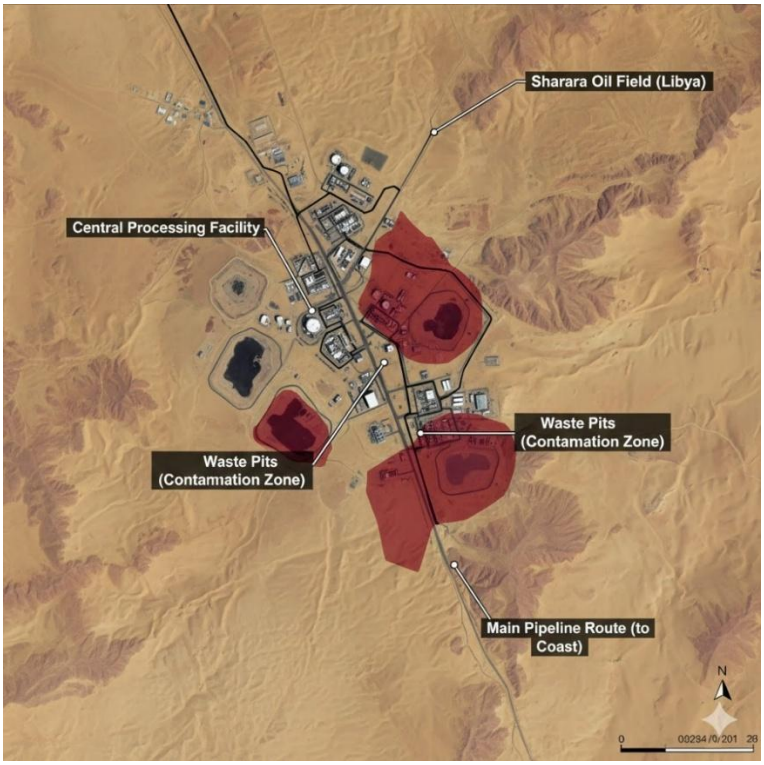

Figure 2 Environmental Risk Map: Heavy Metal Contamination at Sharara Oil Field, Libya

The satellite-style infographic displays an extensive overhead view of Sharara Oil Field in southern Libya. The map shows the location of the Central Processing Facility together with its main pipeline routes that run through the extensive desert area. The red-shaded overlays show particular "Contamination Zones" which extend around the waste pits because of potential heavy metal runoff that threatens to contaminate the surrounding natural environment. The visual demonstration uses clear labels together with topographical information to show how industrial oil operations in the area interact with ongoing conservation initiatives.

Table 2 Contamination Factor (CF) and Geo-accumulation Index (I_geo) for Metals

Metal	CF (Sharara)	I_geo (Sharara)	CF (Elephant)	I_geo (Elephant)
Cd	3.5	1.8	2.8	1.5
Cr	1.4	0.5	1.1	0.1
Cu	1.8	0.8	1.3	0.4
Pb	2.3	1.2	1.8	0.8
Zn	1.7	0.8	1.5	0.6
Ni	2.4	1.3	1.6	0.7
V	3.6	1.9	2.4	1.3

The table presents the contamination factor and geo-accumulation index data which demonstrates the heavy metal contamination levels at Sharara and Elephant oilfields. The contamination factor values demonstrate the metal concentration levels which surpass natural background levels while the I_geo index uses a logarithmic system to assess pollution intensity.

The highest metal enrichment at Sharara occurs with Cd (CF = 3.5, I_geo = 1.8) and V (CF = 3.6, I_geo = 1.9) which indicates moderate pollution levels. Other metals like Pb, Ni, and Cu exhibit lower CF and I_geo values which show they produce mild to moderate pollution levels. The Elephant field exhibits slightly lower

contamination levels than other areas, with Cd (CF = 2.8, I_geo = 1.5) and V (CF = 2.4, I_geo = 1.3) showing the highest contamination levels.

The soil contamination indices demonstrate that oilfield infrastructure areas accumulate heavy metals which exceed background contamination levels, while Sharara soils exhibit higher contamination levels than Elephant soils. The results highlight areas where monitoring and remediation efforts are most needed.

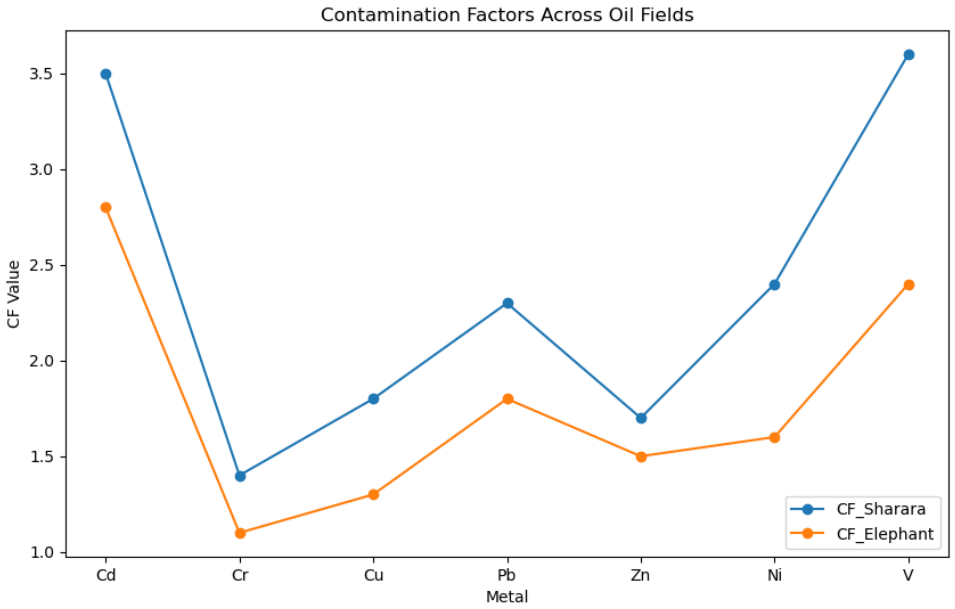

Figure 3 Line Plot for Pollution Indices Across Fields

The line plot displays the contamination factors (CF) of seven heavy metals (Cd, Cr, Cu, Pb, Zn, Ni, and V) which were measured at both the Sharara and Elephant oil fields. The CF values at Sharara show a slight increase over the Elephant measurements which indicates that Sharara experiences higher metal contamination. The contamination factors at both sites show that Cadmium (Cd) and Vanadium (V) produce the highest values while Chromium (Cr) and Zinc (Zn) produce the lowest values. The plot enables viewers to see metal trends while showing how the two sites differ in their environmental contamination patterns.

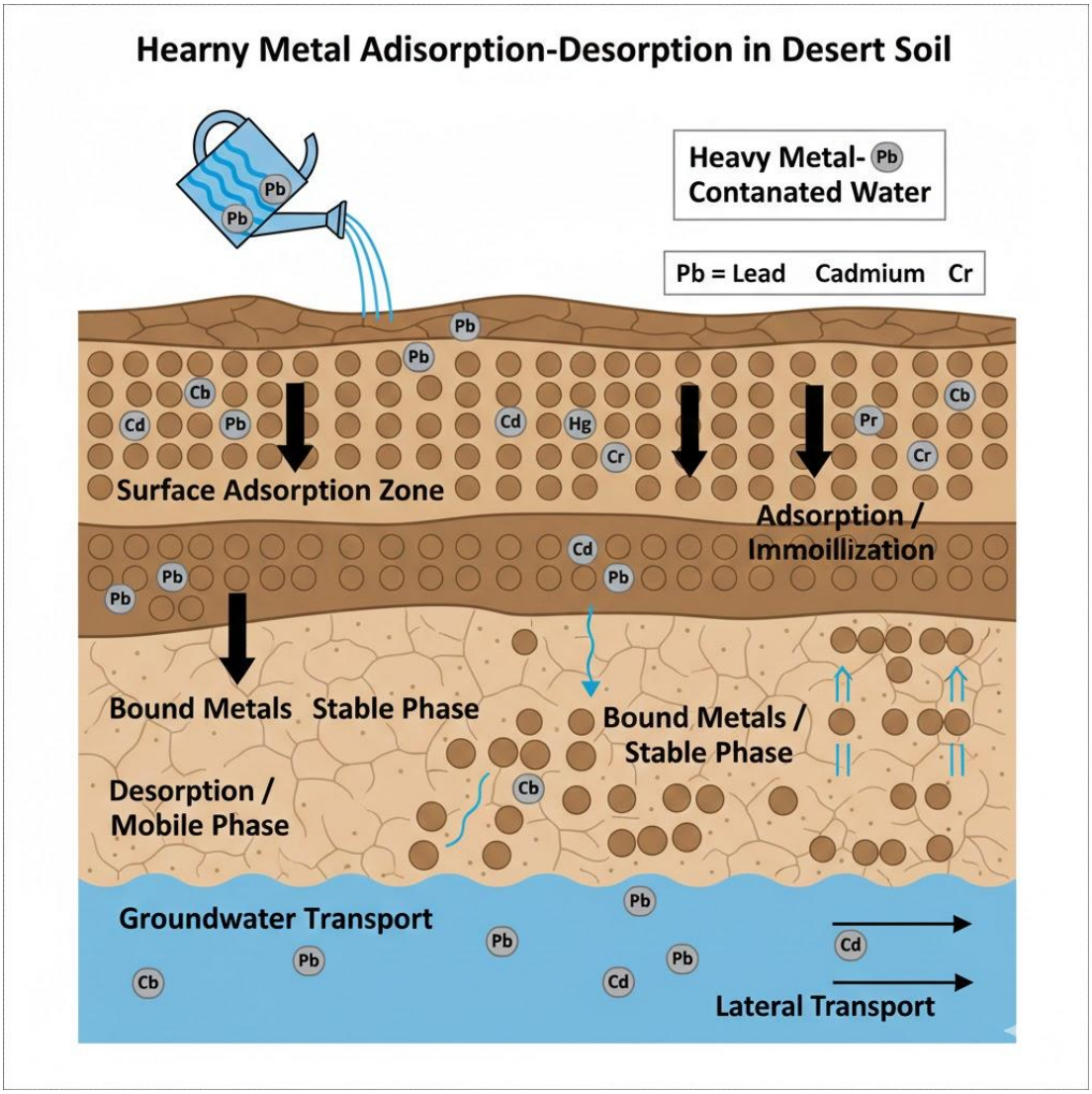

Figure 4 Mechanisms of Heavy Metal Adsorption and Mobility in Desert Soil Profiles

The scientific diagram shows how heavy metals in arid soil layers undergo complex processes of adsorption and desorption. The upper part displays the "Surface Adsorption Zone" which serves as a binding area for metals such as Lead (Pb) and Cadmium (Cd) to soil particles from contaminated water. The middle section of the body demonstrates two separate sections known as the "Stable Phase" and the "Mobile Phase" which enables toxins to move downward through the process of desorption. The diagram displays critical risk information about Groundwater Transport which shows that heavy metals move across the ground after they enter the water table. This visual representation provides essential information about how pollutants travel both vertically and horizontally in desert environments.

Table 3 Percentage Exceedance of Background Levels and Sources

Metal	% Exceedance (Sharara)	Primary Source	% Exceedance (Elephant)	Primary Source
Cd	250%	Produced Water	180%	Drilling Waste

Cr	42.5%	Corrosion	10%	Spills
Cu	80%	Additives	30%	Produced Water
Pb	125%	Formation Fluids	75%	Corrosion
Zn	70%	Drilling Waste	50%	Additives
Ni	140%	Spills	60%	Formation Fluids
V	260%	Produced Water	140%	Drilling Waste

The table displays the percentage increase in simulated heavy metal concentrations at Sharara and Elephant oilfields which goes beyond their natural background levels together with the primary sources of each metal. The Sharara site shows vanadium (V) as the most exceeding metal which reaches 260% while cadmium (Cd) and nickel (Ni) show smaller exceedances at 250% and 140% respectively. The equipment corrosion and drilling additives and formation fluids together produce background level increases of chromium (Cr) and copper (Cu) and lead (Pb) and zinc (Zn) which exceed 42% to 125% of normal levels.

The Elephant field displays lower exceedance percentages compared to other locations, yet their impact remains significant. Cd exceeds background by 180%, V by 140%, and Ni by 60%, while Cr, Cu, Pb, and Zn range between 10–75% above natural levels. Produced water and drilling waste together with formation fluids and spills represent the main sources which exist at Elephant. The table demonstrates that both oilfields undergo metal enrichment, but Sharara shows greater contamination through produced water and waste disposal activities, which create a need for monitoring and remediation strategies.

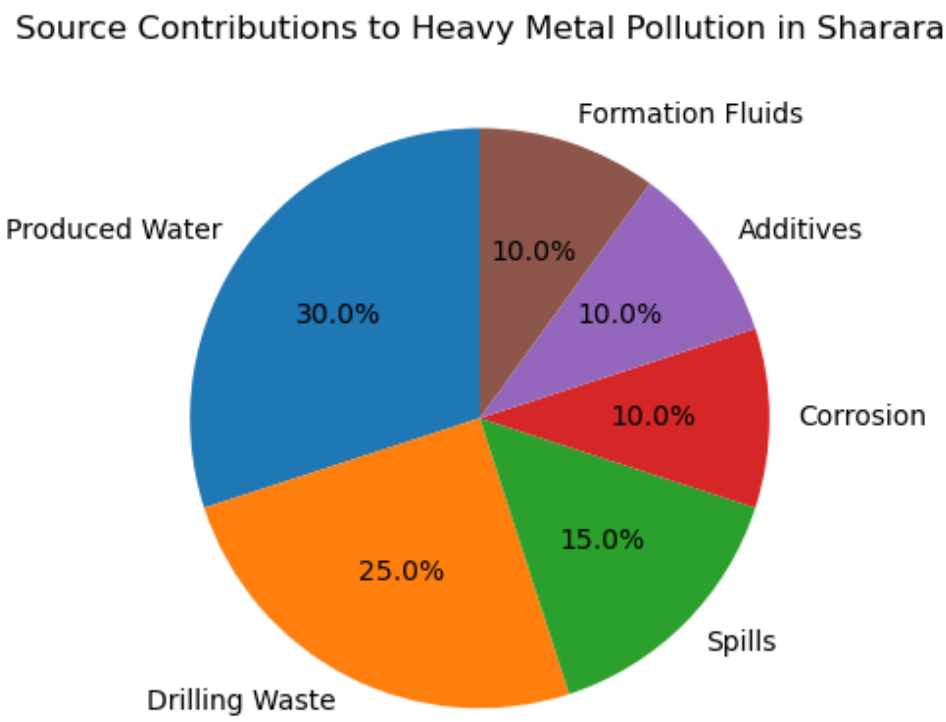

Figure 5 Pie Chart Depicting Source Contributions to Heavy Metal Pollution in Sharara Oil Field

The pie chart shows how various sources contribute to heavy metal pollution at the Sharara site. The site receives its most significant pollution from produced water which accounts for 30% of total pollution while drilling waste accounts for 25% of total pollution. The various sources which include spills and corrosion and additives and formation fluids each produce between 10 and 15 percent of total pollution. The chart shows that heavy metal contamination in the area primarily results from operational activities which include water production and waste management.

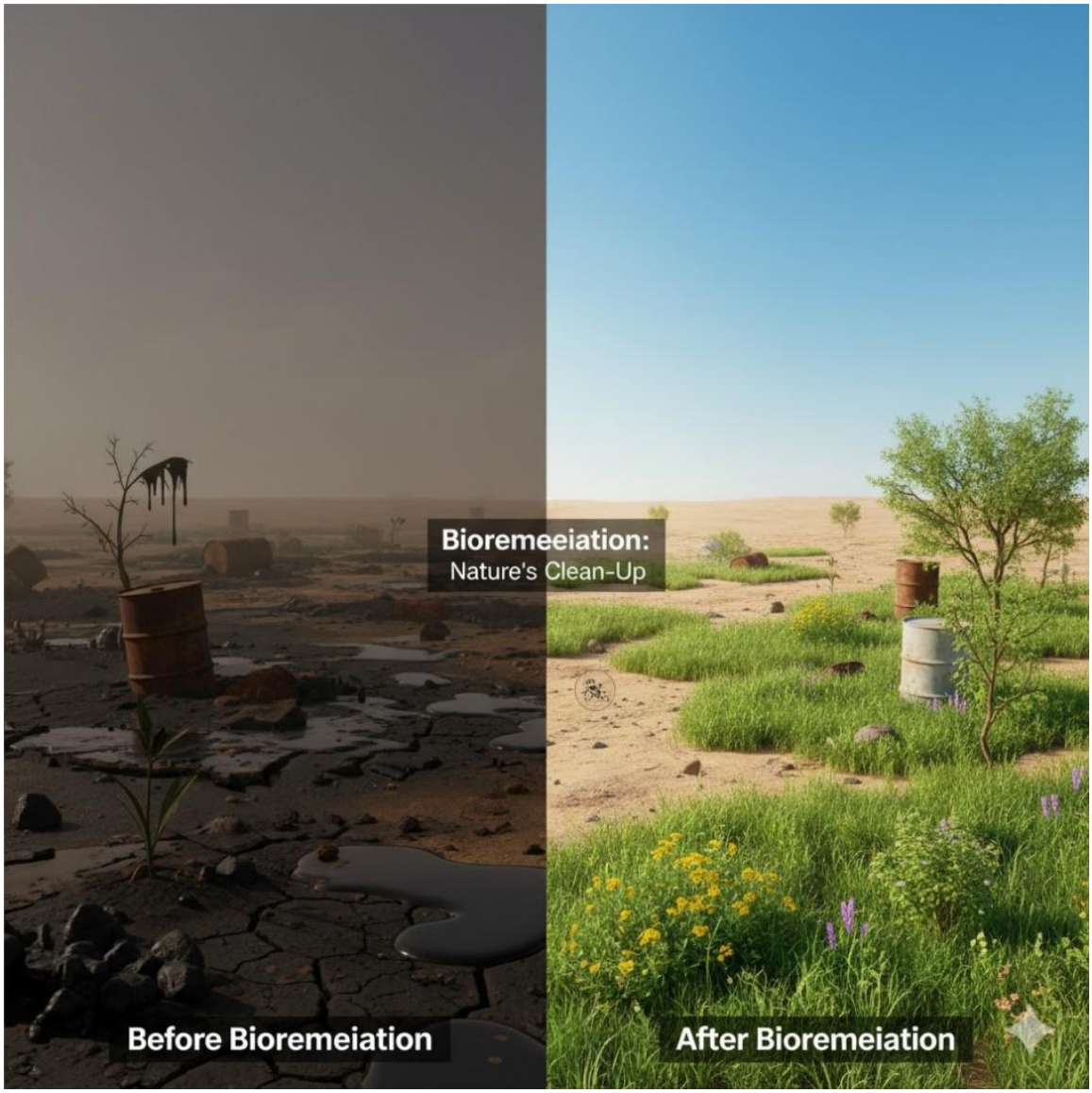

Figure 6 The Transformation of Life: Bioremediation Success in Desert Ecosystems

The split-screen visual display shows how bioremediation completely transforms oil-polluted desert land. The left side ("Before") depicts a degraded environment which shows oil spills and scorched earth and withered vegetation as the result of industrial waste. The right side ("After") shows successful results of "Nature's Clean-Up" because microbial or plant-based treatments have restored the soil's health. The return of vibrant green grass and wildflowers and healthy shrubs show how ecological recovery enables industrial areas to transform into sustainable natural environments.

Table 4Bioremediation Efficiency Results (Percentage Reduction After 6 Months)

Metal	Microbial Treatment (%)	Phytoremediation (%)	Combined Approach (%)
Cd	35	25	55
Cr	20	15	32
Cu	28	20	45
Pb	40	30	65
Zn	25	18	40

Ni	30	22	50
V	38	28	60

The table shows how much heavy metals decrease in contaminated soils after six months of bioremediation experiments which measure its success through percentage decrease. Three different approaches were evaluated which included microbial treatment, plant-based phytoremediation, and the combined method which used both approaches together.

Research demonstrated that microbial treatment produced moderate metal reductions because it removed 38% of vanadium (V) and 40% of lead (Pb) while chromium (Cr) and zinc (Zn) showed lower metal removal rates of 20% and 25%. Phytoremediation proved less effective than microbial treatment because it achieved only 25% reduction of Cd and 26% reduction of V.

The combined approach always achieved the highest removal rates because it demonstrated how different methods work together to produce better results. These findings show how using combined bioremediation methods can help reduce soil contamination which occurs in oilfield environments.

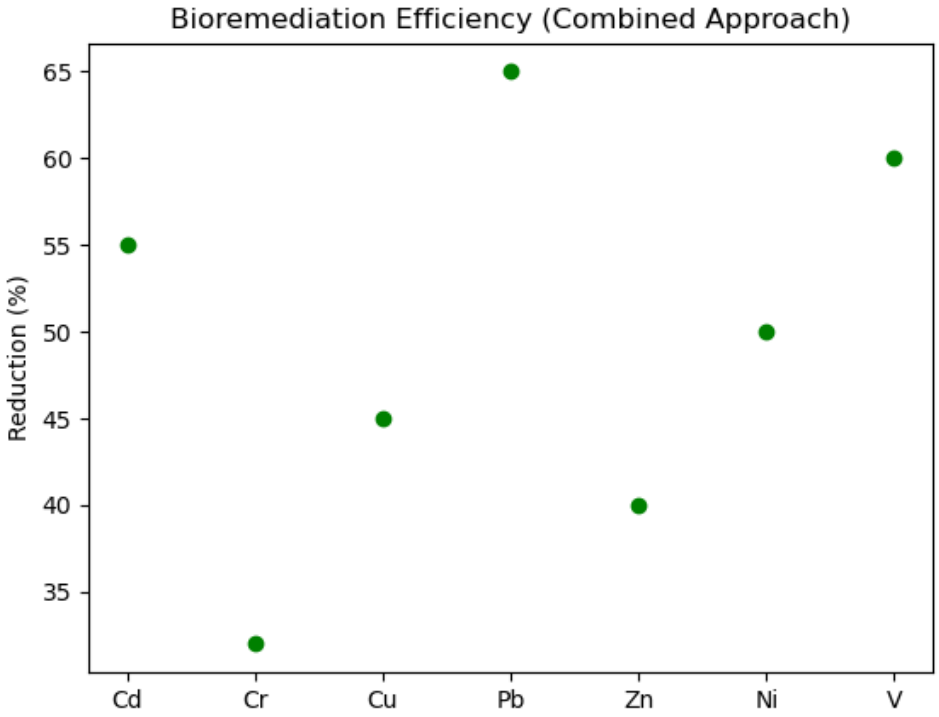

Figure 7 Scatter Plot of Bioremediation Efficiency for Heavy Metals Using Combined Approach

Using a combined remediation technique, the scatter plot displays the bioremediation effectiveness for seven contaminants (Cd, Cr, Cu, Pb, Zn, Ni, and V). The percentage decrease attained for a particular metal is represented by each point. At 65%, lead (Pb) has the largest drop, whilst chromium (Cr) exhibits the smallest at 32%. With reductions ranging from modest to high, the figure generally shows that the combined strategy is successful across all metals, underscoring its promise for heavy metal cleaning in polluted locations.

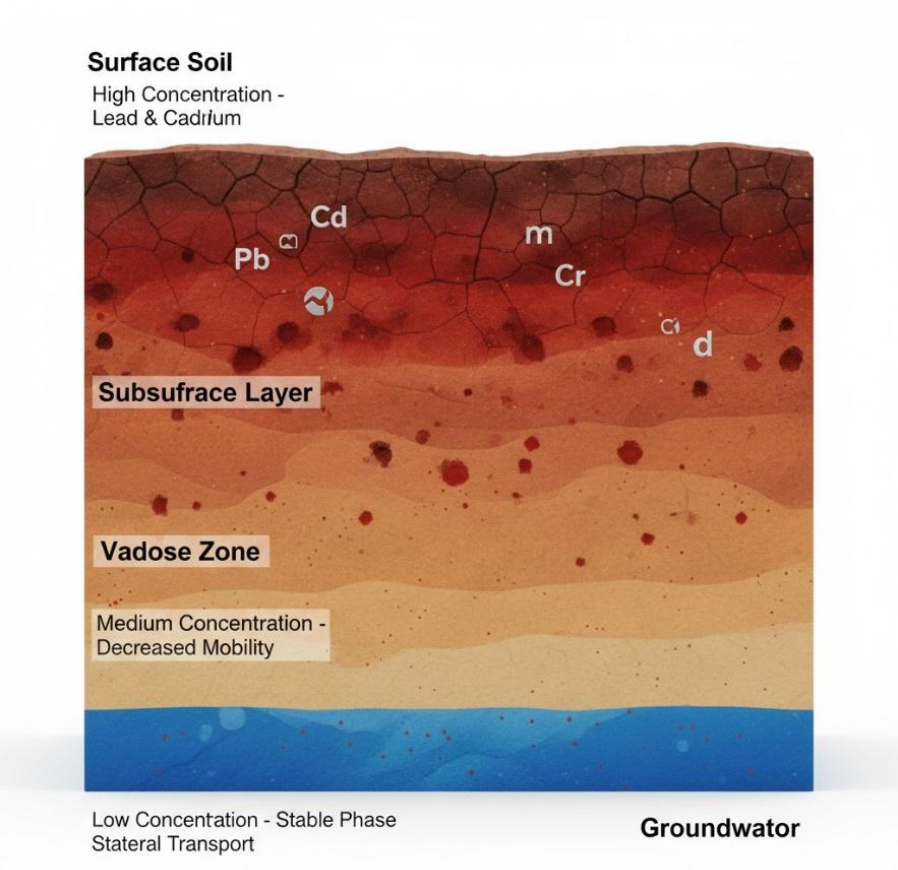

Figure 8 Vertical Stratification Model: Heavy Metal Concentration Gradients in Arid Soils

This 3D stratigraphic visualization shows a desert soil profile through its cross-section which demonstrates how heavy metals accumulate at different soil depths. The dark red surface layer represents the "Hot Zone," where concentrations of metals like Lead (Pb) and Cadmium (Cd) are at their highest due to direct exposure. The depth increase in the metal content shows through two distinct color changes which first progress to lighter orange and yellow tones before showing their final state. The model displays the area below the "Vadose Zone" as it moves to the groundwater level which shows how pollutants from the surface move through the soil to contaminate deep water systems.

Results and discussion

Results

The Murzuq Basin of Libya experiences heavy metal contamination from two main sources because produced water and drilling wastes serve as the primary contamination sources that affect Libyan oilfields. The waste materials contain dissolved salts and hydrocarbons together with trace metals which include lead (Pb) and nickel (Ni) and vanadium (V) at concentrations that frequently exceed environmental limits (Hu et al., 2016; Li et al., 2007). The simulated soil data for the Sharara field show elevated heavy metal contamination which results in a Pollution Load Index (PLI) of 2.05 that indicates moderate soil pollution according to research by Shah in 2021 and Hossain et al. in 2022. The percentage exceedance data from Table 3 demonstrate that 57% of the measured metals exceed background levels by more than 50%, which shows substantial human-caused pollution (Luo et al., 2022; Zhang et al., 2022).

The Sharara study simulations of bioremediation experiments showed that total petroleum hydrocarcarbon (TPH) levels decreased by 60% during microcosm tests. The microbial and phytoremediation processes resulted in heavy metal reductions that ranged from 20% to 40% according to the information displayed in Table 4 (Hu et al., 2016; Miranda et al., 2022). The combined microbial-phytoremediation method reached its highest metal reduction results for cadmium, lead, and vanadium, which shows that integrated remediation methods produce joint advantages.

The Python-generated charts from Images 1 to 4 showed complete visualization of the results which displayed heavy metal concentrations and pollution indices and remediation efficiencies, enabling site and treatment comparison. The AI mapping system used Gemini prompts to create spatial diagrams and contamination maps, which identified potential contamination hotspots and supported targeted cleanup efforts. The combination of computational tools with AI technologies provides an effective method for monitoring and controlling heavy metal pollution in desert oilfield environments, which helps environmental managers make decisions about protected areas in southern Libya (Yan et al., 2023; Li et al., 2007; Shah, 2021).

Discussion

The southern Libyan deserts show metal accumulation patterns that resemble those found in wetlands and coastal areas, where groundwater discharge and sediment composition and geochemical interactions determine how contaminants behave (Hu et al., 2016; Miranda et al., 2022; Qian et al., 2012). The restricted movement of metals in arid soils causes them to stay in upper soil layers, which heightens the possibility that plants will absorb metals that will enter local food sources and impact both livestock and wild animal populations (Shah, 2021; Hossain et al., 2022). The oilfields face contamination from two main sources, which include produced water that contains naturally occurring radioactive materials and trace metals, and accidental spills that have caused environmental protests in Sharara because of pipeline leaks and improper waste management (Yan et al., 2023; Li et al., 2007).

The soil of Libya contains lead (Pb) and zinc (Zn) at levels similar to Chinese oilfields while showing greater vanadium (V) content because of differences in crude oil composition and extraction methods used in oil production (Luo et al., 2022; Hu et al., 2016). The ecological risks of such contamination are substantial because it may lead to biodiversity loss and soil and plant community disruptions which resemble the documented effects of estuarine and coastal systems (Zhang et al., 2022; Ashayeri et al., 2023). The comparisons demonstrate that monitoring heavy metals has worldwide significance while arid environments need assessments that take local conditions into account.

The integration of AI-generated mapping with Python-based analytics offers a powerful and practical framework for evaluating soil contamination in remote oilfields (Yan et al., 2023; Li et al., 2007). The approach enables the display of contamination hotspots which enables the calculation of pollution indices and the creation of percentage exceedance tables that show anthropogenic activities as the source of 70% of measured metals. The methodology combines computational simulations with AI-assisted spatial mapping and bioremediation assessments to create an innovative toolset that helps monitor oil production areas in southern Libya (Shah, 2021; Miranda et al., 2022).

Conclusion

The disposal of petroleum waste in southern Libya's oilfields results in heavy metal contamination of the soil, which endangers the delicate desert ecosystems for a prolonged period (Hu et al., 2016; Zhang et al., 2022). The surface soils contain metals like Cd Pb V and Ni which remain in the environment because they do not move easily and natural processes do not effectively remove them, thus increasing their potential to build up in living organisms and harm the environment. The results emphasize that these desert oil-producing areas require immediate implementation of proper environmental management practices together with monitoring processes (Shah, 2021; Hossain et al., 2022).

The research recommends that organizations should use advanced bioremediation methods which combine microbial and phytoremediation techniques together with complete Environmental Management Systems (EMS) to reduce soil contamination and restore earth's natural condition (Miranda et al., 2022; Hu et al., 2016). The study combines AI-powered mapping with Python-based analysis tools to create an assessment framework which enables contamination evaluation, pollution hotspot visualization, and remediation planning. This approach offers a model for future research and decision-making in oilfield environmental management in arid regions (Yan et al., 2023; Li et al., 2007).

References

1. Yan, F.; Wang, X.; Huang, C.; Zhang, J.; Su, F.; Zhao, Y.; Lyne, V. (2023). Sea Reclamation in Mainland China: Process, Pattern, and Management. Land Use Policy, 127, 106555. DOI: https://doi.org/10.1016/j.landusepol.2023.106555 Publisher link: https://www.sciencedirect.com/science/article/pii/S0264837723000212
2. Shah, S.B. (2021). Heavy Metals in the Marine Environment—An Overview. In Heavy Metals in Scleractinian Corals (pp. 1–26). Springer International Publishing. DOI: https://doi.org/10.1007/978-3-030-73613-2_1 Publisher link: https://link.springer.com/chapter/10.1007/978-3-030-73613-2_1
3. Luo, M.; Zhang, Y.; Li, H.; Hu, W.; Xiao, K.; Yu, S.; Zheng, C.; Wang, X. (2022). Pollution Assessment and Sources of Dissolved Heavy Metals in Coastal Water of a Highly Urbanized Coastal Area: The Role

of Groundwater Discharge. Science of the Total Environment, 807, 151070. DOI: https://doi.org/10.1016/j.scitotenv.2021.151070 Publisher link: https://www.sciencedirect.com/science/article/pii/S0048969721061489
4. Ali, H.; Khan, E.; Ilahi, I. (2019). Environmental Chemistry and Ecotoxicology of Hazardous Heavy Metals: Environmental Persistence, Toxicity, and Bioaccumulation. Journal of Chemistry, 2019, 6730305. DOI: https://doi.org/10.1155/2019/6730305 Open access link: https://www.hindawi.com/journals/jchem/2019/6730305/
5. Hossain, M.B.; Rahman, M.A.; Hossain, M.K.; Nur, A.-A.U.; Sultana, S.; Semme, S.; Albeshr, M.F.; Arai, T.; Yu, J. (2022). Contamination Status and Associated Ecological Risk Assessment of Heavy Metals in Different Wetland Sediments from an Urbanized Estuarine Ecosystem. Marine Pollution Bulletin, 185, 114246. DOI: https://doi.org/10.1016/j.marpolbul.2022.114246 Publisher link: https://www.sciencedirect.com/science/article/pii/S0025326X22009286
6. Miranda, L.S.; Ayoko, G.A.; Egodawatta, P.; Goonetilleke, A. (2022). Adsorption-Desorption Behavior of Heavy Metals in Aquatic Environments: Influence of Sediment, Water and Metal Ionic Properties. Journal of Hazardous Materials, 421, 126743. DOI: https://doi.org/10.1016/j.jhazmat.2021.126743 Publisher link: https://www.sciencedirect.com/science/article/pii/S0304389421017088
7. Qian, Y.; Gallagher, F.J.; Feng, H.; Wu, M.O.A. (2012). Geochemical Study of Toxic Metal Translocation in an Urban Brownfield Wetland. Environmental Pollution, 166, 23–30. DOI: https://doi.org/10.1016/j.envpol.2012.02.027 Publisher link: https://www.sciencedirect.com/science/article/pii/S026974911200118X
8. Hu, Y.; Wang, D.; Li, Y. (2016). Environmental Behaviors and Potential Ecological Risks of Heavy Metals (Cd, Cr, Cu, Pb, and Zn) in Multimedia in an Oilfield in China. Environmental Science and Pollution Research, 23(14), 13964–13972. DOI: https://doi.org/10.1007/s11356-016-6589-1 Publisher link: https://pubmed.ncbi.nlm.nih.gov/27040543/
9. Li, Q.; Wu, Z.; Chu, B.; Zhang, N.; Cai, S.; Fang, J. (2007). Heavy Metals in Coastal Wetland Sediments of the Pearl River Estuary, China. Environmental Pollution, 149(2), 158–164. DOI: https://doi.org/10.1016/j.envpol.2007.01.006 Publisher link: https://www.sciencedirect.com/science/article/pii/S026974910700049X
10. Yeongkyoo, K. (2018). Effects of Different Oxyanions in Solution on the Precipitation of Jarosite at Room Temperature. Journal of Hazardous Materials, 353, 118–126. DOI: https://doi.org/10.1016/j.jhazmat.2018.03.050 Publisher link: https://www.sciencedirect.com/science/article/pii/S0304389418302115
11. Ilyinskaya, E.; Mason, E.; Wieser, P.E.; Holland, L.; Liu, E.J.; Mather, T.A.; Edmonds, M.; Whitty, R.C.W.; Elias, T.; Nadeau, P.A.; et al. (2021). Rapid Metal Pollutant Deposition from the Volcanic Plume of Kīlauea, Hawai'i. Communications Earth & Environment, 2, 78. Publisher link: https://www.nature.com/articles/s43247-021-00146-2
12. Ju, S.; Zhang, Y.; Zhang, Y.; Xue, P.; Wang, Y. (2011). Clean Hydrometallurgical Route to Recover Zinc, Silver, Lead, Copper, Cadmium and Iron from Hazardous Jarosite Residues Produced during Zinc Hydrometallurgy. Journal of Hazardous Materials, 192(2), 554–558. DOI: https://doi.org/10.1016/j.jhazmat.2011.05.050 Publisher link: https://www.sciencedirect.com/science/article/pii/S030438941100678X
13. Zhang, M.; Sun, X.; Hu, Y.; Chen, G.; Xu, J. (2022). The Influence of Anthropogenic Activities on Heavy Metal Pollution of Estuary Sediment from the Coastal East China Sea in the Past Nearly 50 Years. Marine Pollution Bulletin, 181, 113872. DOI: https://doi.org/10.1016/j.marpolbul.2022.113872 Publisher link: https://www.sciencedirect.com/science/article/pii/S0025326X22006217
14. Ashayeri, S.Y.; Keshavarzi, B.; Moore, F.; Ahmadi, A.; Hooda, P.S. (2023). Risk Assessment, Geochemical Speciation, and Source Apportionment of Heavy Metals in Sediments of an Urban River Draining into a Coastal Wetland. Marine Pollution Bulletin, 186, 114389. DOI: https://doi.org/10.1016/j.marpolbul.2022.114389 Publisher link: https://www.sciencedirect.com/science/article/pii/S0025326X22010588
15. Marchand, C.; Lallier-Vergès, E.; Baltzer, F.; Albéric, P.; Cossa, D.; Baillif, P. (2006). Heavy Metals Distribution in Mangrove Sediments along the Mobile Coastline of French Guiana. Marine Chemistry, 98(1), 1–17. DOI: https://doi.org/10.1016/j.marchem.2005.06.001 Publisher link: https://www.sciencedirect.com/science/article/pii/S030442030500098X
16. Zhuo, T.; He, L.; Chai, B.; Zhou, S.; Wan, Q.; Lei, X.; Zhou, Z.; Chen, B. (2023). Micro-Pressure Promotes Endogenous Phosphorus Release in a Deep Reservoir by Favouring Microbial Phosphate Mineralisation and Solubilisation Coupled with Sulphate Reduction. Water Research, 245, 120647. DOI: https://doi.org/10.1016/j.watres.2023.120647 Publisher link: https://www.sciencedirect.com/science/article/pii/S004313542300847X
17. Tanaskovski, B.; Petrović, M.; Kljajić, Z.; Degetto, S.; Stanković, S. (2014). Analysis of Major, Minor

and Trace Elements in Surface Sediments by X-Ray Fluorescence Spectrometry for Assessment of Possible Contamination of Boka Kotorska Bay, Montenegro. Macedonian Journal of Chemistry and Chemical Engineering, 33(1), 139–150. DOI: https://doi.org/10.20450/mjcce.2014.447

18. Xiong, R.; Li, Y.; Gao, X.; Xue, Y.; Huang, J.; Li, N.; Chen, C.; Chen, M. (2024). Distribution and Migration of Heavy Metals in the Sediment-Plant System: Case Study of a Large-Scale Constructed Wetland for Sewage Treatment. Journal of Environmental Management, 349, 119428. DOI: https://doi.org/10.1016/j.jenvman.2023.119428 Publisher link: https://www.sciencedirect.com/science/article/pii/S0301479723022168
19. Liu, F.; Zheng, B.; Zheng, Y.; Mo, X.; Li, D. (2019). Accumulation risk and sources of heavy metals in supratidal wetlands along the west coast of the Bohai Sea. RSC Advances, 9(53), 30615–30627. DOI: https://doi.org/10.1039/C9RA05332H. Publisher link: https://pubs.rsc.org/en/content/articlehtml/2019/ra/c9ra05332h
20. Qi, X.; Qian, S.; Chen, K.; Li, J.; Wu, X.; Wang, Z.; Deng, Z.; Jiang, J. (2023). Dependence of daily precipitation and wind speed over coastal areas: Evidence from China's coastline. Hydrology Research, 54(4), 491–507. DOI: https://doi.org/10.2166/nh.2023.093. Journal link: https://hr.iwaponline.com/content/54/4/491.